NASA TN D-1434

NASA TN D-1434

c. 1

TECHNICAL NOTE

D-1434

MONTE CARLO CALCULATIONS OF NEUTRON NUMBER SPECTRA AND BUILDUP FACTORS IN INFINITE CONICAL CONFIGURATIONS

By Millard L. Wohl

Lewis Research Center
Cleveland, Ohio

NATIONAL AERONAUTICS AND SPACE ADMINISTRATION

WASHINGTON September 1962

NATIONAL AERONAUTICS AND SPACE ADMINISTRA]

TECHNICAL NOTE D-1434

MONTE CARLO CALCULATIONS OF NEUTRON NUMBER SPECTRA AND BUILDUP FACTORS IN INFINITE CONICAL CONFIGURATIONS

By Millard L. Wohl

SUMMARY

A Monte Carlo code simulating neutron transport in infinite cones of water and water-equivalent hydrogen was prepared for an IBM 704 computer. The code was essentially a modification of the point-source, infinite-medium code used in NASA TN D-850.

Studies were made of differential neutron number spectra and associated buildup factors for infinite cones having apex half-angles of 15°, 30°, 45°, and 60°. The buildup factors obtained were compared with those for the appropriate infinite medium, which allowed an examination of the effect of solid angle subtended by material on the transport of 6-Mev source neutrons emanating from the cone apex.

The variation of number buildup factor with distance for the various cones shows that neutron scattering out of the cones is predominant in the first 30 to 40 centimeters of material, and that transport beyond this distance is of a similar nature in all the cones.

INTRODUCTION

The problem of calculating required neutron and gamma-ray shielding for the crew compartment and components of a nuclear-powered space vehicle is a very formidable one. Prospective configurations for such shielding requirements consist of various arrays of finite geometric shapes of material.

Most of the radiation attenuation properties of plausible shielding materials have been described in terms of spatially and energy-dependent number and energy spectra and corresponding buildup factors for point-source, infinite-medium configurations (see refs. 1 and 2). This type of information is not directly useful in the calculation of actual shields, but can provide, at best, coarse upper bounds for the true spectra and buildup factors, which may lead to gross overestimation of shielding requirements.

A geometric arrangement that closely resembles an actually proposed "shadow shield" is the infinite cone. For the work reported herein, the infinite-medium code of reference 1 is modified for application to infinite conical media. Neutron number spectra and buildup factors for a variety of infinite cones of water and water-equivalent hydrogen are computed by the Monte Carlo method - digital computer simulation of particle transport - at various depths of penetration from a 6-Mev point source located at the apex of the cone; the number spectra are normalized to correspond to the infinite-medium results (ref. 1). Such information can provide useful correlations between number buildup factors and solid angle of shielding material subtended at particular surfaces in the attenuating medium. These correlations may provide more realistic upper limits for number spectra and buildup factors in deep-penetration-neutron-shielding calculations for actual configurations.

E-1584

SYMBOLS

A	typical first collision point
a	biasing parameter
B_N	number buildup factor
DR	distance between collisions, cm
E	neutron energy, Mev
EBIAS	importance sampling cutoff energy, Mev
ECUT	individual case history termination energy, Mev
E_α	(n,α) process threshold energy, Mev
IDBUG	neutron parametric debugging output control number
IDUMP	dump reading control number
K	normalization constant for source-neutron probability density function
MODF	equals zero when second argument is integral multiple of first argument
NCHIS	current cumulative number of case histories
NDUMP	number of case histories between periodic dumps
NFIN	number of case histories at which calculation is complete

N_o	differential number flux, neutrons/(cm^2)(sec)(Mev)
O	origin of coordinate system
$\overline{OA}$	typical initial flight path (fig. 1)
p	source-neutron-polar-angle probability density function
R	uniformly distributed pseudorandom number in $0 \rightarrow 1$ interval
r	penetration depth, cm
SL	sense light
s^*	probability density function for χ
WT	neutron weight after collision
XSECT	cross section
X,Y,Z	Cartesian coordinates
β	cone apex half-angle, deg
δ	source-neutron-direction polar angle, deg
ρ	distance between collision point and scoring shell along flight path, cm
Σ	macroscopic neutron interaction cross section
σ	microscopic neutron interaction cross section
φ	source-neutron azimuthal angle (fig. 1), deg
χ	nonuniformly distributed pseudorandom number in $0 \rightarrow 1$ interval

Subscripts:

NEW	after collision
(n,α)	refers to neutron interaction producing an alpha particle
OLD	before collision
t	total

tH total hydrogen

tO total oxygen

Superscript:

' dummy variable of integration

ANALYSIS AND PROCEDURE

The Monte Carlo code digitally simulates neutron transport in infinite cones of water and water-equivalent hydrogen (hydrogen having the same density as that in water). A great saving in computing time is effected if neutrons are contained, as well as is feasible, within the cones, since it is only these neutrons that make substantial contributions to the deep penetration fluxes and buildup factors. Good containment is accomplished by biasing the source-neutron directions and the polar scattering angles at primary and all subsequent collisions by use of modified probability density functions.

Geometry and Transport Mechanics

A conventional three-dimensional Cartesian coordinate system with the source point located at the origin is used to specify collision positions. The conical infinite transport media have their apexes at the origin and open symmetrically about the positive z-axis (fig. 1). The polar and azimuthal angles of the velocity vector and the energy complete the phase specification of the neutron in transport.

For computing efficiency and convenience, source neutrons are emitted at a rate of 1 per second and are given an initial direction within the cone of material under consideration in the following manner. If the source is assumed to be isotropic, the probability density function that describes the emergence of a neutron within the cone at an angle δ with the z-axis is

$$p(\delta) = \frac{K}{2} \sin \delta \tag{1}$$

where K is a constant of normalization. The normalization condition is

$$\frac{K}{2} \int_0^\beta \sin \delta \, d\delta = 1 \tag{2}$$

where β is the cone apex half-angle. From equation (2) it follows that

$$K = \frac{2}{1 - \cos \beta} \tag{3}$$

It is apparent from equation (2) that K is the fraction of a neutron per increment of $\cos \delta$ that yields proper source normalization within the cone and essentially maps an infinite-medium, isotropic-source distribution into a similar distribution for an infinite cone. Thus $1/K$ is a weight factor to be attached to each source neutron. A choice of initial polar angle δ is made in the conventional manner (ref. 1) by the use of X, an element of a set of nonuniformly distributed pseudorandom numbers in the 0 to 1 interval:

$$\int_0^{\delta} p(\delta')d\delta' = \frac{K}{2}\int_0^{\delta} \sin \delta' \, d\delta' = \frac{1}{1 - \cos \beta}\int_0^{\delta} \sin \delta' \, d\delta' = X \tag{4}$$

The probability density function for X is

$$s^*(X) = \frac{1 - e^{-a}}{a\left[1 - (1 - e^{-a})X\right]} \tag{5}$$

This choice of X (ref. 1) forces crowding of source particle directions toward the z-axis and thus improves the overall computational efficiency of the program, since fewer neutrons physically escape from the cone in the early stages of case histories than would be removed if uniformly distributed random numbers were used directly. As in reference 1, the values of X are obtained from values of a uniformly distributed random number R by the transformation

$$X = \frac{1 - e^{-aR}}{1 - e^{-a}} \tag{6}$$

where a is a real positive adjustable parameter. Another weight correction factor $1/s^*(X)$ must now be applied to the source neutron (see ref. 1), since the nonuniformly distributed pseudorandom numbers X are used. Hence, the weight to be attached to a source neutron is

$$\frac{1}{Ks^*(X)} = \frac{1 - \cos \beta}{2} \frac{a\left[1 - (1 - e^{-a})X\right]}{1 - e^{-a}} \tag{7}$$

The core of the Monte Carlo calculation procedure is identical with that used in reference 1. Neutron flux is computed with the use of statistical estimation by counting neutrons, weighted a priori by $e^{-\Sigma_t \rho}$, "incident" on a test sphere of unit cross-sectional area at the desired spherical-flux-recording-shell radius. The subroutine of reference 1 used to accomplish this computation was appropriately modified to account for the conical geometry. The fluxes are normalized to the infinite-medium results by multiplying by the normalization factor.

$$\frac{4\pi}{2\pi(1 - \cos \beta)} = \frac{2}{1 - \cos \beta} \tag{8}$$

E-1584

which is the reciprocal of the fraction of all space subtended by an infinite cone and, because of the particular mode of normalization chosen, is identical to K (eq. (3)).

In the water-cone calculations, (n,α) oxygen absorption is accounted for by multiplying the neutron weight by $1 - \frac{\sigma(n,\alpha)}{\sigma_t}$; oxygen cross sections of reference 3 were used. In the hydrogen-cone calculations, no absorption occurs. In both cases, neutron histories are terminated by means of a cutoff energy of 0.4 Mev. For each cone considered, 2500 neutron case histories were executed; typical computing time for a case was 40 minutes.

In addition to reducing polar scattering angles by the exponential biasing technique previously mentioned, neutron transit distances were lengthened to favor deep penetration. The X-set of pseudorandom numbers was used to accomplish this also, the transit distance being $DR = -\frac{1}{\Sigma_t} \ln(1 - X)$; the appropriate weight correction is made here also. Figure 2 is the flow diagram from which the code was written.

For purposes of comparison with infinite-medium buildup factors computed from the results of reference 1, all cross sections for hydrogen and oxygen, including the oxygen elastic differential scattering cross section, were computed using tables obtained from references 3 and and 4. The buildup factors plotted in figure 3 were computed from the number spectra of figure 4 and from the definition of buildup factor

$$B_N = \frac{\int_{0.4}^{6-\epsilon} 4\pi r^2 N_o(r,E)\, dE}{e^{-\Sigma_t r}} + 1 \quad \text{for } \epsilon = 0.001 \tag{9}$$

from reference 1.

E-1584

DISCUSSION OF RESULTS

The number spectra for the water cones (figs. 4(a) to (d)) reflect the effects of oxygen scattering, as did the infinite-medium spectra of reference 1. The two most visible effects are the relative maximums at 5.25 and 2.25 Mev. These are due, respectively, to first scatterings from oxygen nuclei and the large antiresonance in the oxygen total cross section located at approximately 2.3 Mev. The number spectra for the hydrogen cones (figs. 4(e) to (h)) display a more monotonic average behavior with large fluctuations, particularly at low energies, that are mainly statistical in nature. When neutrons have experienced several collisions, as those contributing to the low-energy bins, statistical fluctuations due to the rough nature of the importance sampling technique employed are particularly evident.

The number buildup factors for the water and hydrogen cones (fig. 3) rise with increasing penetration depth, which is to be expected. For a particular depth, these quantities increase with increasing cone apex half-angle; this is due to the larger amount of multiple scattering as the cone angle and cross-sectional diameter increase.

A particularly interesting aspect of the curves of figure 3 is the fact that the rates of change of the buildup factors with penetration depth are highly divergent within the first 30 to 40 centimeters. This displays the increasing importance of scattering out of the cones with decreasing cone angle and cross-sectional diameter, where multiple scattering effects are diminished. The roughly parallel behavior of the buildup-factor curves at penetration depths greater than 60 centimeters implies that neutron scattering out of the cones at the deeper penetrations is of relatively similar importance for all the cones.

The ratio of the infinite-medium to 15° cone number buildup factors in water (fig. 3(a)) is as large as 18. For water-equivalent hydrogen, this ratio has a maximum value of approximately 5.

SUMMARY OF RESULTS

Neutron number fluxes and buildup factors in various infinite cones of water and water-equivalent hydrogen were computed by means of a Monte Carlo code written for the IBM 704 computer. A 6-Mev point source at the cone apex was used. The following are the results of interest:

1. The differential number spectra in water display the high-energy-oxygen first scattering peak and the 2.3-Mev peak because of the large oxygen total cross section antiresonance at that energy.

2. The infinite-cone number buildup factors in water and hydrogen exhibit a rise with increasing distance and are as small as 1/18 of the infinite-medium buildup factors.

3. The mode of variation of number buildup factor with penetration depth indicates the importance of neutron scattering out of the cones at shallow penetrations; this effect is especially strong for the small-angle-cone cases.

E-1584

Lewis Research Center
National Aeronautics and Space Administration
Cleveland, Ohio, June 29, 1962

REFERENCES

1. Fessler, Theodore E., and Wohl, Millard L.: Monte Carlo Studies of Gamma-Ray and Neutron Transport in Infinite Homogeneous Media. NASA TN D-850, 1961.

2. Goldstein, Herbert: Fundamental Aspects of Reactor Shielding. Addison-Wesley Publ. Co., Inc., 1959.

3. Goldstein, Herbert: Fast Neutron Data for Oxygen. NDA-Memo-15C-15, AEC, Nov. 3, 1953.

4. Hughes, Donald J., and Schwartz, Robert B.: Neutron Cross Sections. BNL-325, Second ed., Brookhaven Nat. Lab., July 1, 1958.

E-1584

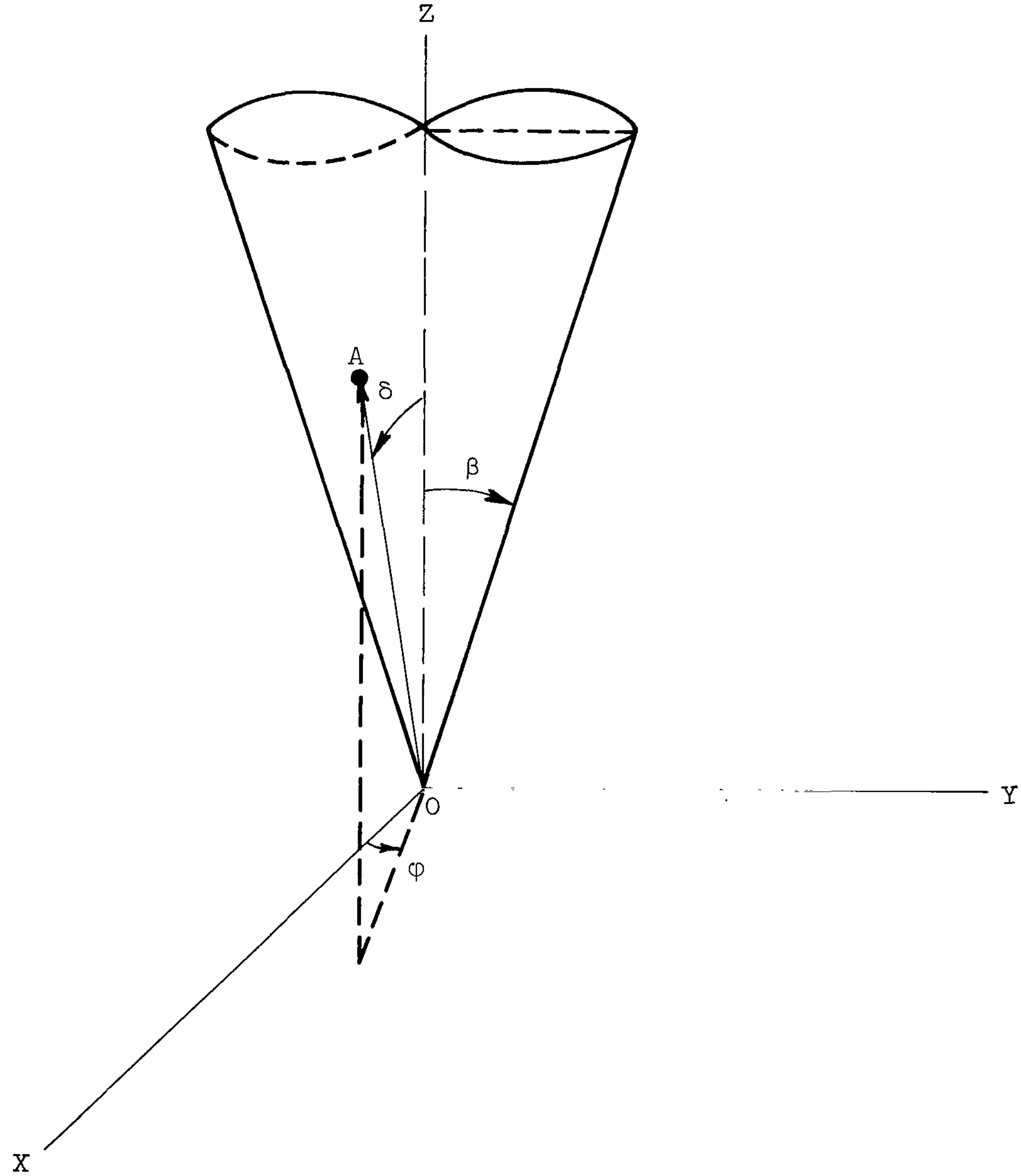

Figure 1. - Coordinate system used to orient infinite cones and to specify collision and flux-shell positions. Source-neutron-direction polar angle less than or equal to cone apex half-angle.

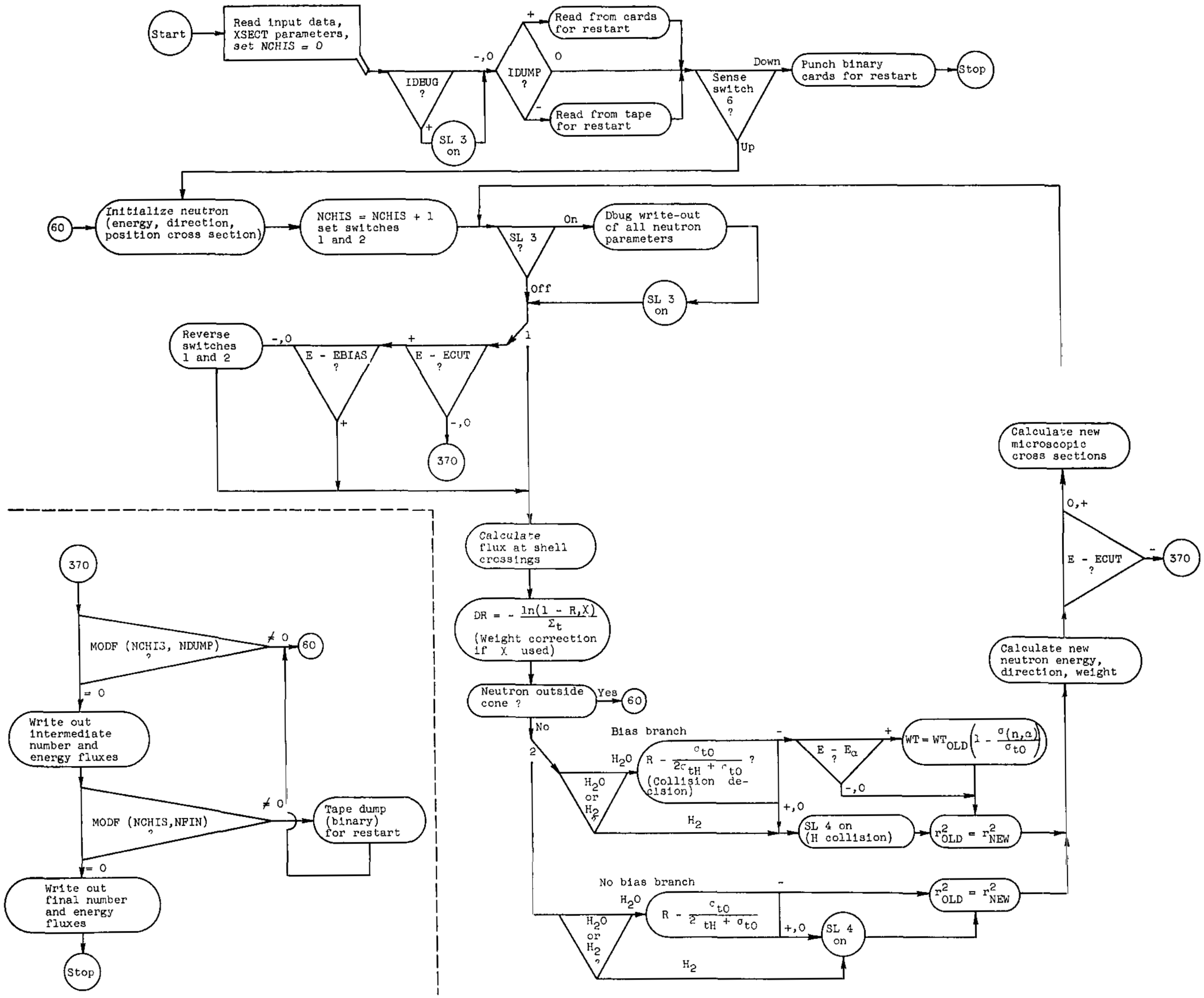

Figure 2. - Flow diagram for Monte Carlo calculation of neutron flux in infinite cones of water and water-equivalent hydrogen.

E-1584

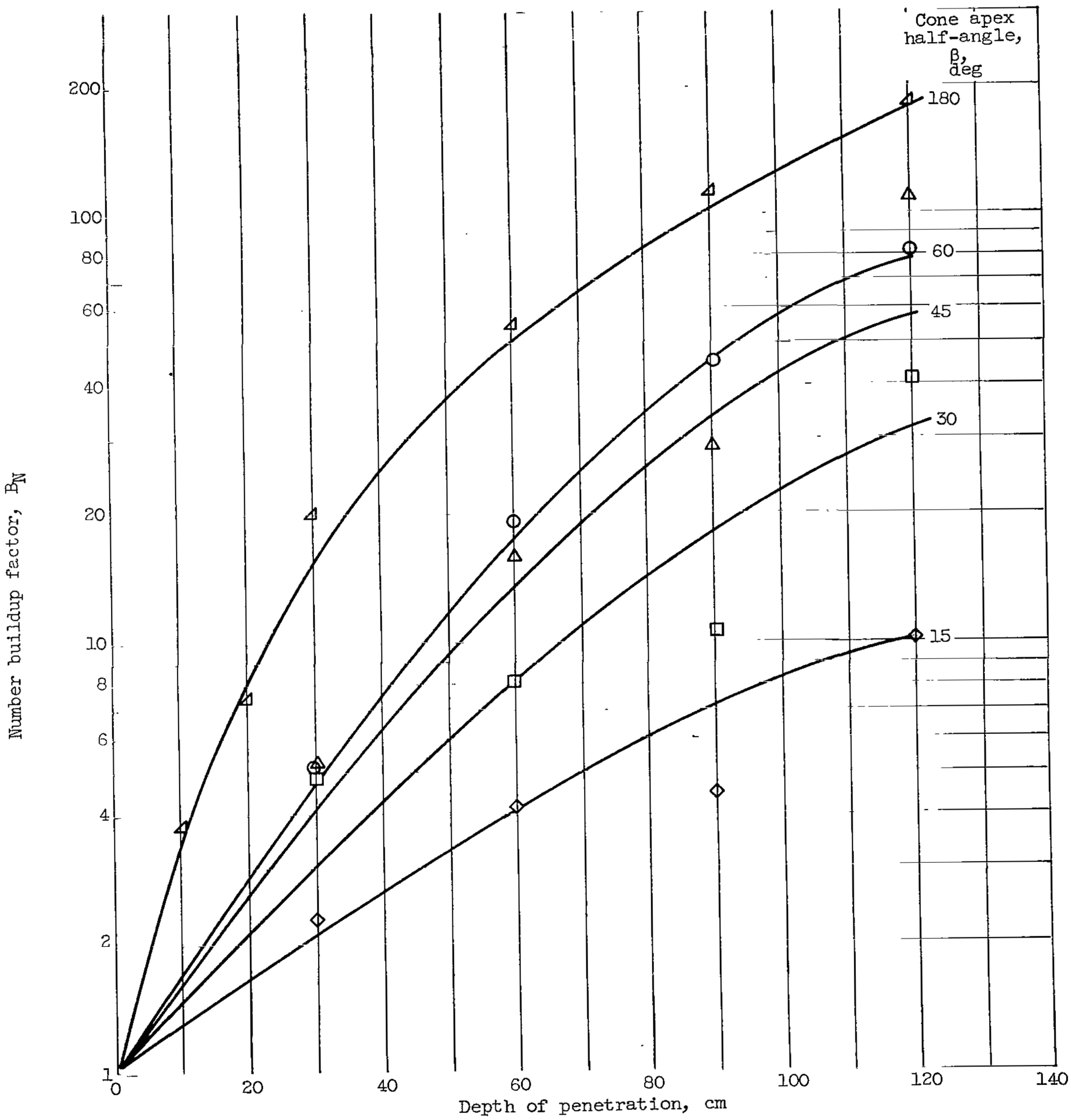

(a) Infinite water cones.

Figure 3. - Variation of number buildup factor with depth of penetration.

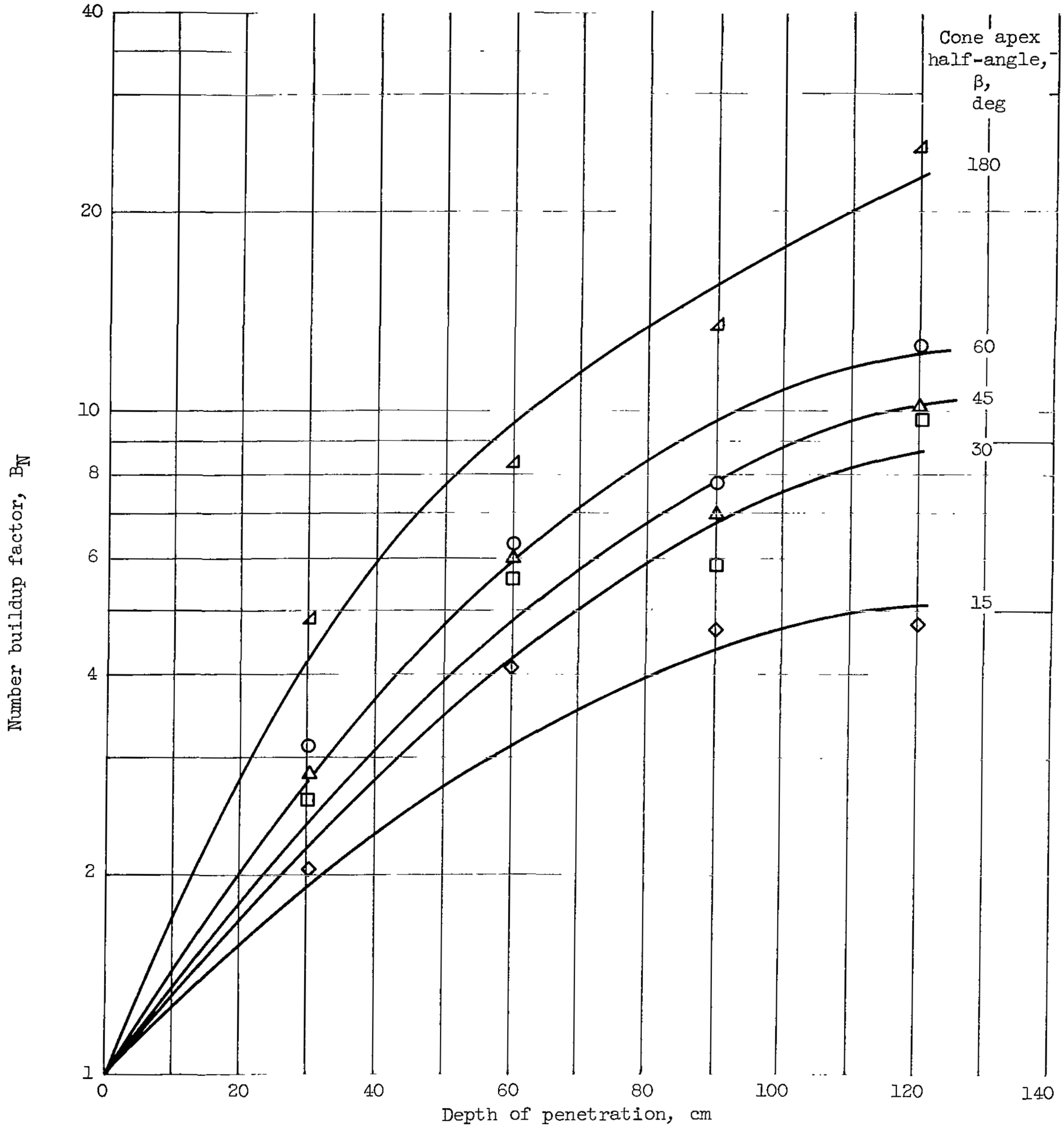

(b) Infinite water-equivalent hydrogen cones.

Figure 3. - Concluded. Variation of number buildup factor with depth of penetration.

E-1584

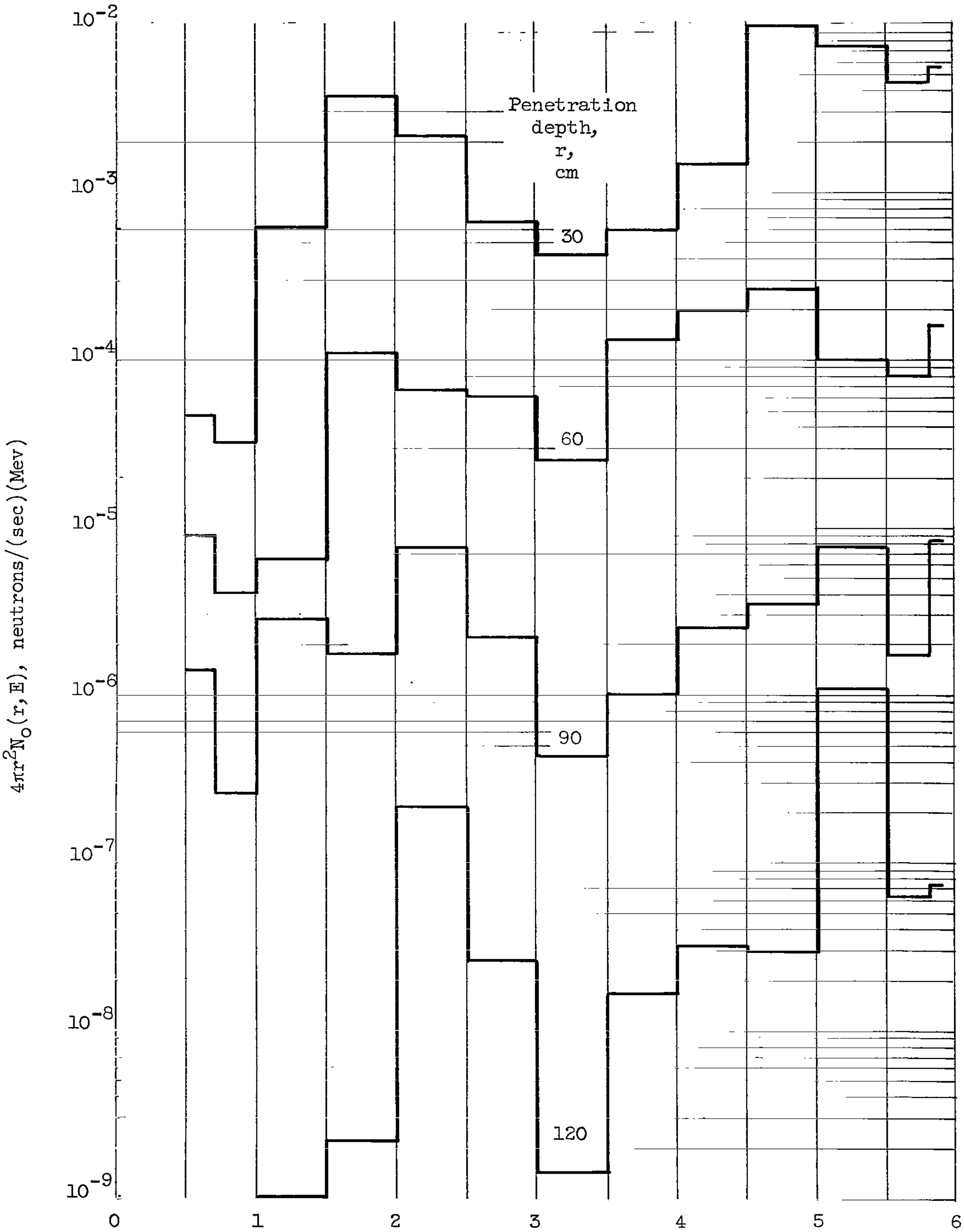

(a) Water cone; apex half-angle, 15°.

Figure 4. - Neutron number spectra.

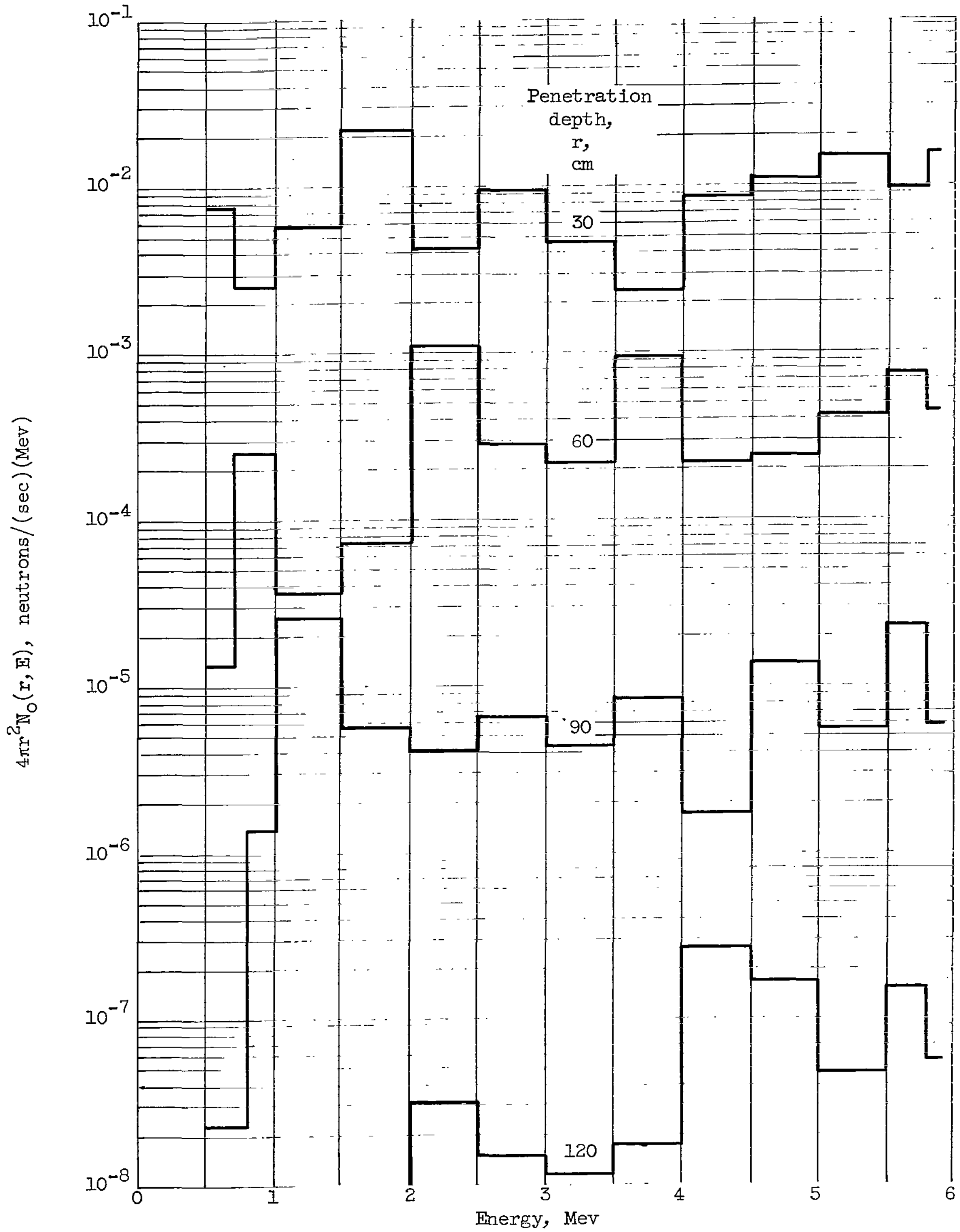

(b) Water cone; apex half-angle, 30°.

Figure 4. - Continued. Neutron number spectra.

E-1584

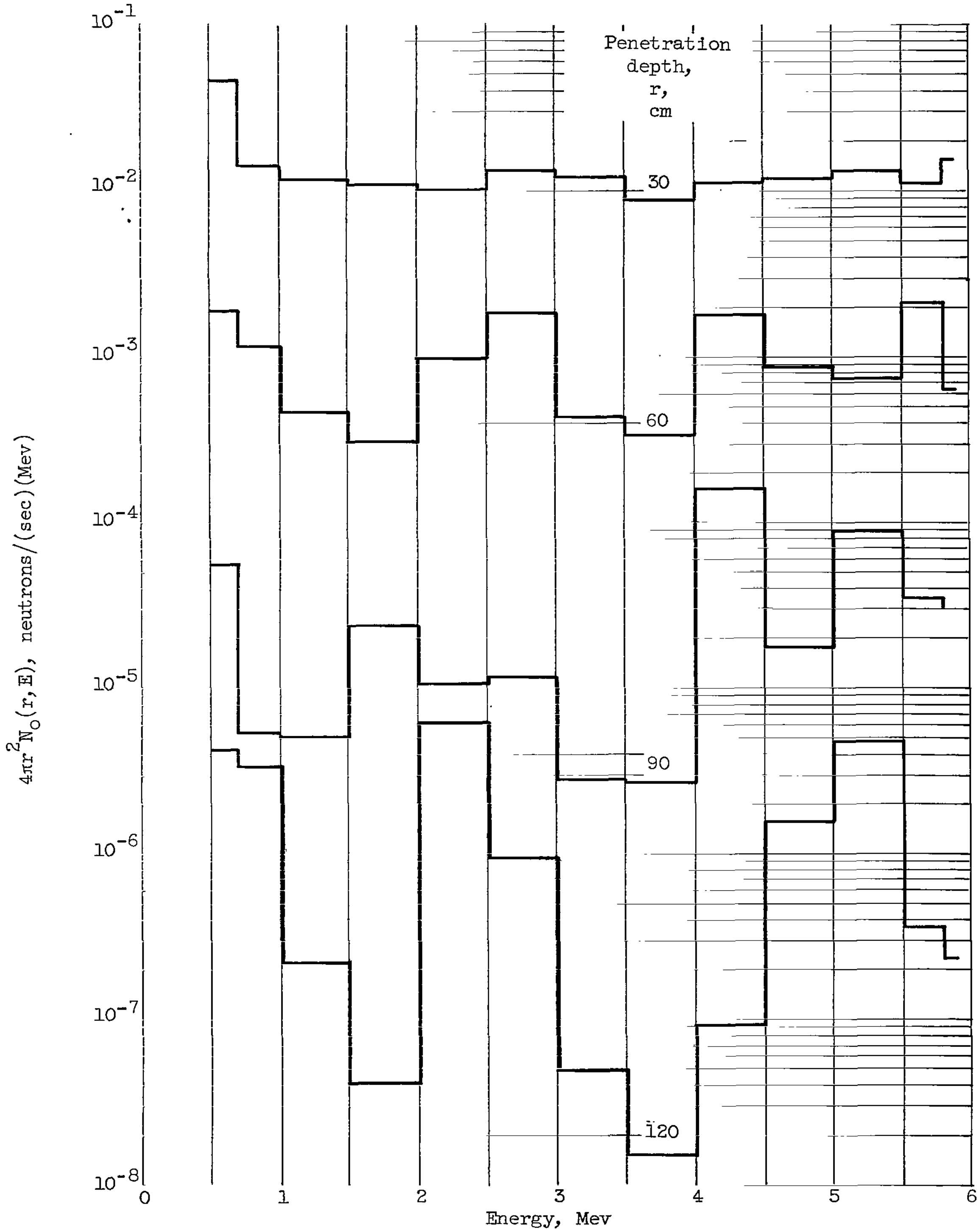

(c) Water cone; apex half-angle, 45°.

Figure 4. - Continued. Neutron number spectra.

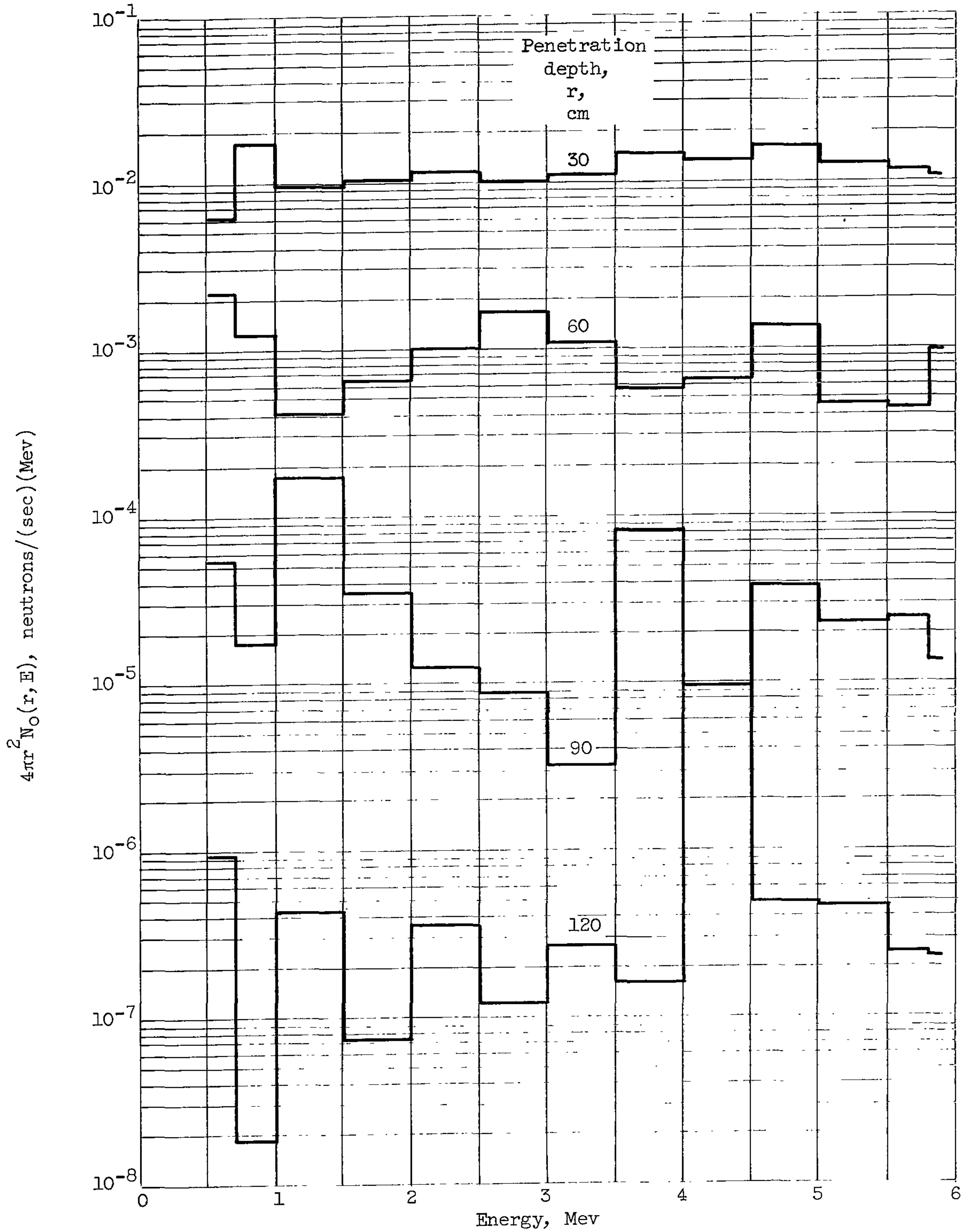

(d) Water cone; apex half-angle, 60°.

Figure 4. - Continued. Neutron number spectra.

E-1584

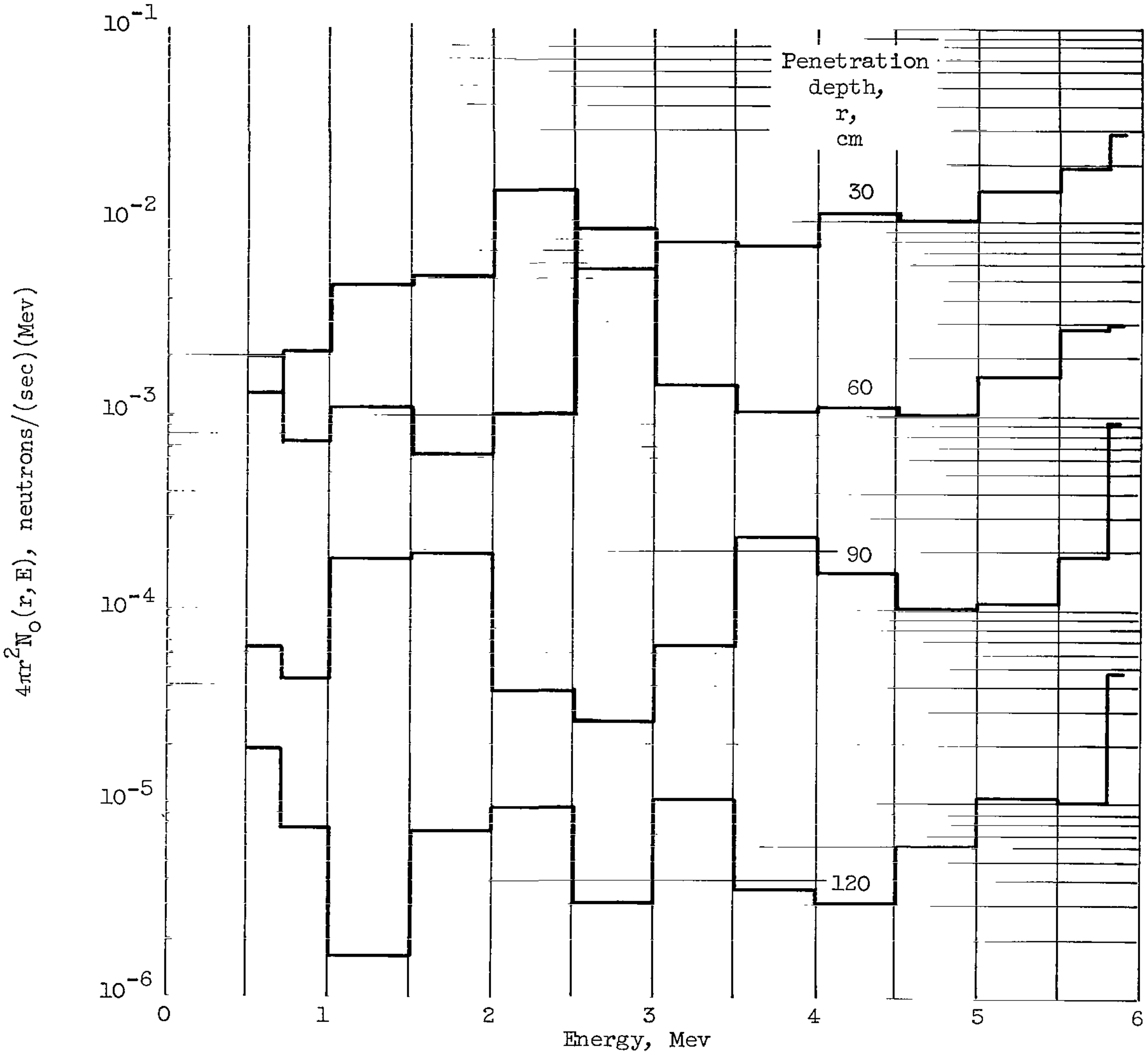

(e) Water-equivalent hydrogen cone, apex half-angle, 15°.

Figure 4. - Continued. Neutron number spectra.

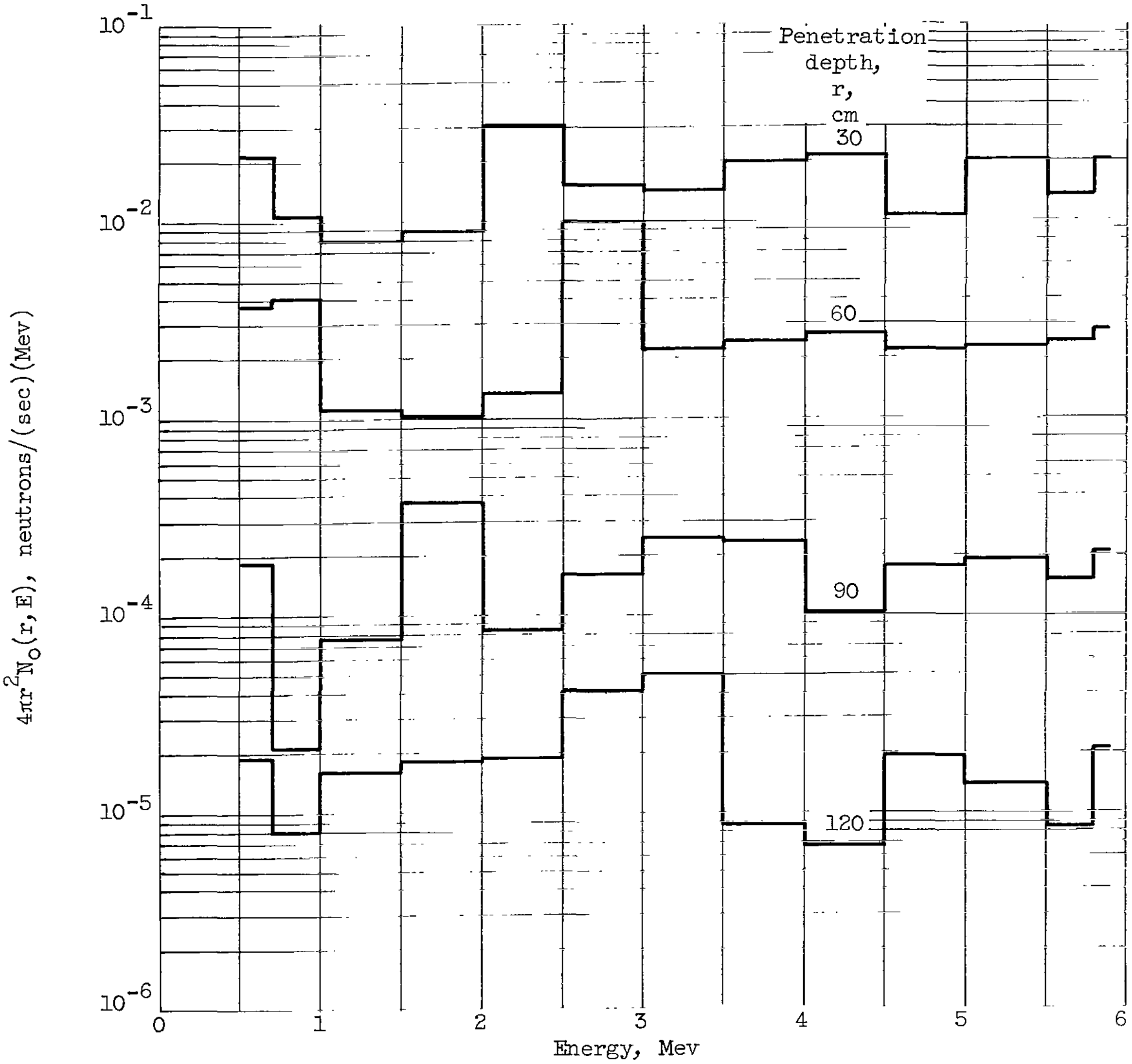

(f) Water-equivalent hydrogen cone; apex half-angle, 30°.

Figure 4. - Continued. Neutron number spectra.

E-1584

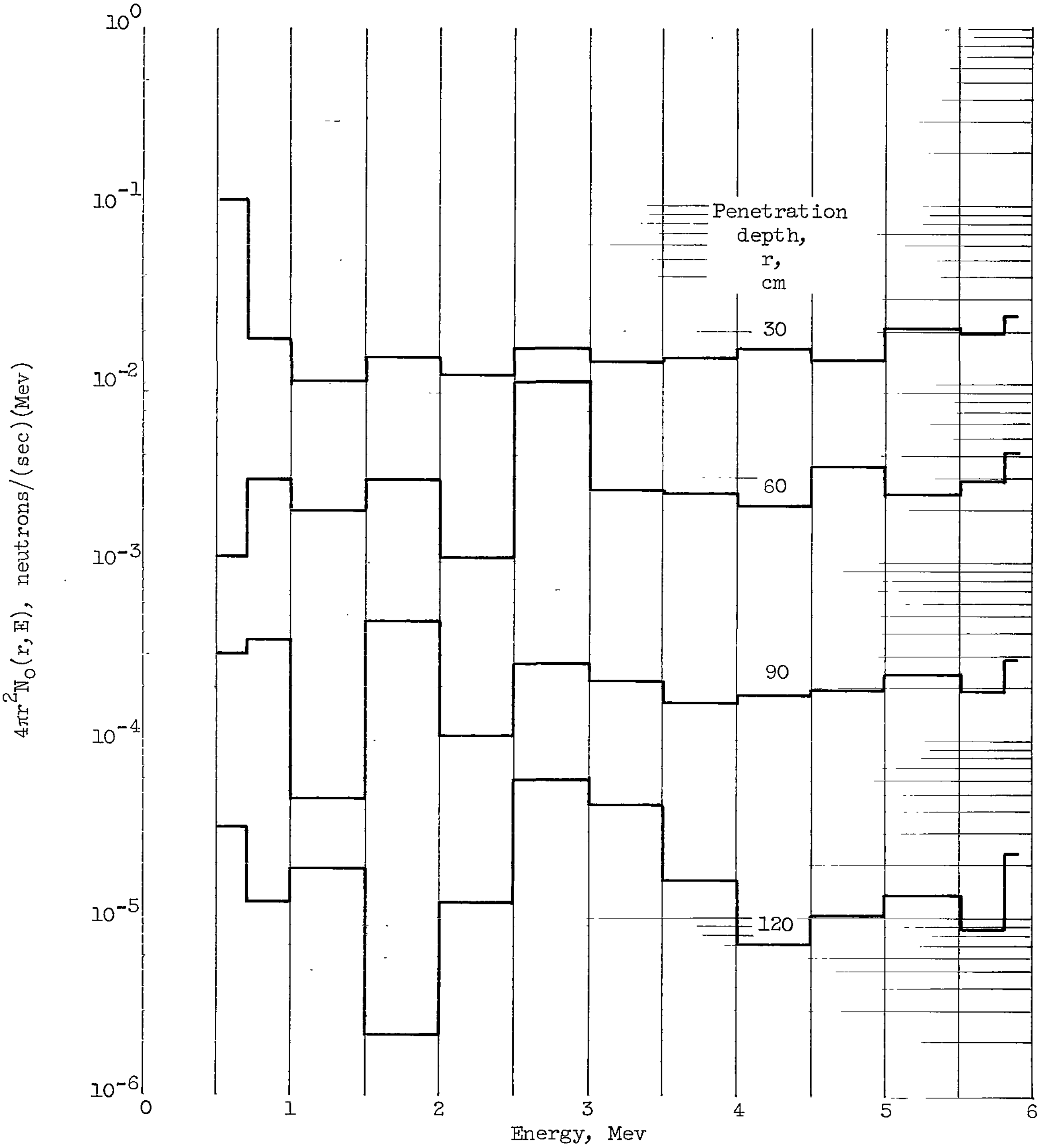

(g) Water-equivalent hydrogen cone; apex half-angle, 45°.

Figure 4. - Continued. Neutron number spectra.

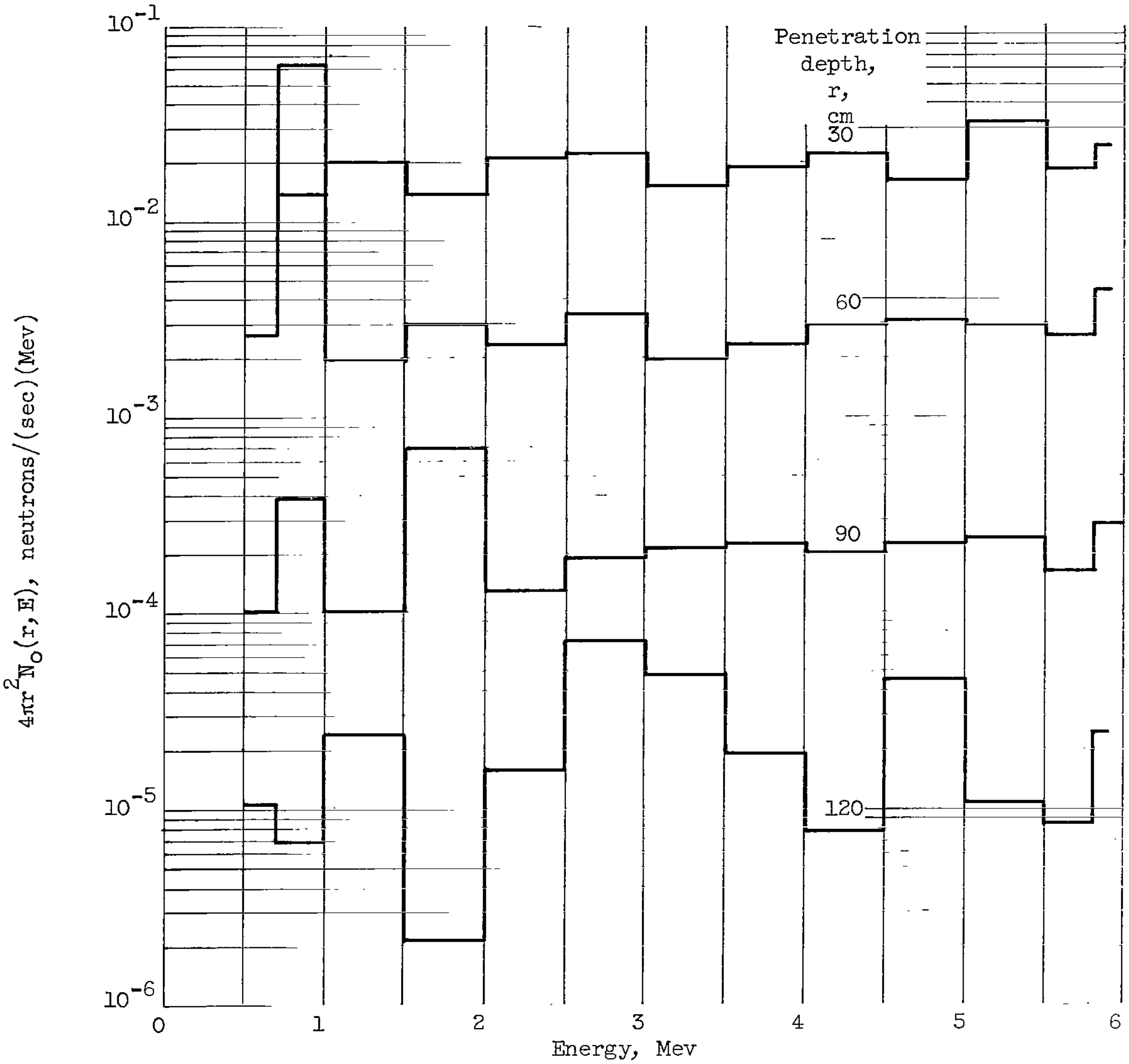

(h) Water-equivalent hydrogen cone; apex half-angle, 60°.

Figure 4. - Concluded. Neutron number spectra.